Cerenkov and radioluminescence imaging of brain tumor specimens during neurosurgery

Antonello Enrico Spinelli
Marco P. Schiariti
Chiara M. Grana
Mahila Ferrari
Marta Cremonesi
Federico Boschi

SPIE.

Cerenkov and radioluminescence imaging of brain tumor specimens during neurosurgery

Antonello Enrico Spinelli,[a,*] Marco P. Schiariti,[b] Chiara M. Grana,[c] Mahila Ferrari,[d] Marta Cremonesi,[d] and Federico Boschi[e]

[a]San Raffaele Scientific Institute, Experimental Imaging Centre, Via Olgettina N. 60, Milan 20182 Italy
[b]Neurological Institute C. Besta, Neurosurgery unit 2, Via Celoria 11, Milano 20133, Italy
[c]European Institute of Oncology, Nuclear Medicine Department, Via Ripamonti 435, Milan 20141, Italy
[d]European Institute of Oncology, Medical Physics Unit, Via Ripamonti 435, Milan 20141, Italy
[e]University of Verona, Department of Computer Science, Strada Le Grazie 15, Verona 37134, Italy

Abstract. We presented the first example of Cerenkov luminescence imaging (CLI) and radioluminescence imaging (RLI) of human tumor specimens. A patient with a brain meningioma localized in the left parietal region was injected with 166 MBq of ^{90}Y-DOTATOC the day before neurosurgery. The specimens of the tumor removed during surgery were imaged using both CLI and RLI using an optical imager prototype developed in our laboratory. The system is based on a cooled electron multiplied charge coupled device coupled with an $f/0.95$ 17-mm C-mount lens. We showed for the first time the possibility of obtaining CLI and RLI images of fresh human brain tumor specimens removed during neurosurgery. © 2016 Society of Photo-Optical Instrumentation Engineers (SPIE) [DOI: 10.1117/1. JBO.21.5.050502]

Cerenkov luminescence imaging (CLI) and radioluminescence imaging (RLI) are becoming well-established methods for preclinical *in vivo* small animal optical imaging, as described in recent reviews.[1–3] CLI and RLI are based, respectively, on the detection of Cerenkov radiation or scintillation light in the visible range. CLI was mainly applied to image the biodistribution of radiopharmaceuticals labeled with beta plus[4–6] and beta minus[7,8] emitters. RLI was developed to obtain the biodistribution of alpha[9] and gamma emitters[10] and can also be used in combination with CLI to enhance the light output.[11]

*Address all correspondence to: Antonello Enrico Spinelli, E-mail: spinelli. antonello@hsr.it

Recent examples of CLI applications to humans were presented in Refs. 12 and 13. In Ref. 12, Cerenkov radiation from the thyroid of a patient treated with ^{131}I for hyperthyroidism was imaged, while Ref. 13 presented an endoscopic Cerenkov luminescence imaging approach to detect gastric cancers in patients injected with 2-[18F]fluoro-2-deoxy-D-glucose.

In this work, we present an application of CLI and RLI for the analysis of *ex vivo* fresh tumor specimens removed during neurosurgery. The main goal of such an approach is to provide a fast molecular imaging estimation of tumor uptake (almost in real time) during surgical procedures. CLI and RLI images were obtained by placing the tumor specimens in an optical imager prototype developed in our laboratory.[14]

The detector used in the prototype is a cooled ($-80°C$) electron multiplied charge coupled device (EMCCD; Andor iXon Ultra) coupled with an $f/0.95$ 17-mm C-mount lens (Schneider Optics). The EMCCD has a back-illuminated 512×512 sensor with pixel size equal to 16 μm, resulting in a detector with total dimensions equal to 8.2×8.2 mm^2.

The smallest achievable field of view (FOV) is $\sim 6.1 \times 6.1$ cm^2, resulting in an image pixel size of 120 μm. To exclude ambient light, the system is mounted on a black light-tight enclosure, in which an adjustable stage is placed for positioning the specimen.

All the CLI and RLI images were acquired using binning = 2 and 5 min of exposure time. A photographic black-and-white image (binning = 2 and exposure time = 0.01 s) was always acquired before any emission image to provide a reference for CLI and RLI. A color image of the sample was also acquired using a conventional camera to show the amount of blood present in the sample.

RLI data were acquired by placing a slab of 1-cm plastic scintillator on top of the specimen. To avoid any contamination, the scintillator was placed ~ 1 mm from the sample. Considering that the plastic scintillator slab is almost transparent, the collected light is thus the sum of Cerenkov and scintillator light produced in the slab. This acquisition scheme (CLI + RLI) was adopted mainly to maximize the light collected by the CCD.

A patient with a grade 1 brain meningioma localized in the left parietal region was injected with 166 MBq of ^{90}Y-DOTATOC the day before surgery. The patient participated in an experimental protocol of a radioguided surgery technique for cerebral tumors with the use of a beta minus radiation probe,[15] which uses ^{90}Y-DOTATOC for diagnostic purposes—contrary to its traditional use with therapeutical quantities for peptide receptor radionuclide therapy. In the new technique in Ref. 15, the ^{90}Y-DOTATOC injected activity is calculated based on a diagnostic positron emission tomography–computed tomography (PET-CT) imaging with the analogue ^{68}Ga-DOTATOC radiopharmaceutical that allows evaluation of the activity concentrations in tumors and thus can establish the activity to be administered for detection with the beta minus probe. In our case, the tumor to nontumor standard uptake value ratio was ~ 25. The required ^{90}Y-DOTATOC activities are of a few hundreds of MBq (typically 185 MBq, 166 MBq in our patient), and the ensuing tumor activity concentrations are also suitable for the study of CLI and RLI.

As shown in Ref. 16, meningiomas express somatostatin receptors; thus, the ^{68}Ga-DOTATOC and ^{90}Y-DOTATOC uptake in the tumor is specific.
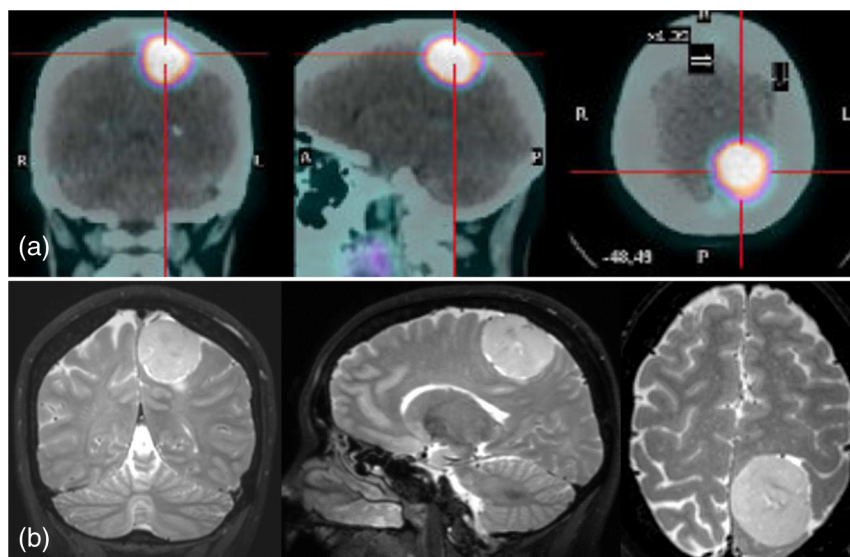
Fig. 1 (a) The coronal, sagittal, and axial PET-CT images of the patient injected with ^{68}Ga-DOTATOC. The PET images were used to estimate the activity concentration of ^{90}Y-DOTATOC in the tumor during surgery. (b) The T2 MR images of the patient acquired without contrast medium.

Figure 1(a) shows the ^{68}Ga-DOTATOC image of our patient, acquired two weeks before surgery. This time is sufficient to guarantee the absence of any interaction between the two radiotracers. A similar time interval was previously considered in a study aimed at comparing the biodistribution of ^{90}Y-DOTATOC in the same patients under two renal protection conditions.[17]

^{68}Ga and ^{90}Y have very different physical half-lives, but the labeling of the same peptide—leading to ^{68}Ga-DOTATOC and ^{90}Y-DOTATOC—allows us to assume similar, if not identical, kinetic processes in tumors and normal organs as well, as applies for ^{111}In-DOTATOC used as a surrogate for ^{90}Y-DOTATOC, as sustained by the joint IAEA, EANM, and SNMMI practical guidance on peptide receptor radionuclide therapy (PRRT).[18] The use of ^{68}Ga-DOTATOC to foresee the outcome of therapy with ^{177}Lu- or ^{90}Y-DOTATOC has been ascertained in the community of PRRT and has been discussed in several papers.[19–22] Moreover, in the protocol of Ref. 15, the presumed activity of ^{90}Y derived from the ^{68}Ga estimates has also been compared with the Monte Carlo simulations of the beta probe sensitivity, showing results in good agreement (data not shown from a paper submitted by Solfaroli Camillocci et al.).

The diagnostic T2 magnetic resonance images of the patient acquired without contrast medium before surgery are shown in Fig. 1(b). The study was approved by the ethical committee of the Carlo Besta Neurological Institute, and informed consent was signed by the patient.

The tumor diameter was ~3.5 cm and the volume was ~18 cm^3. From the DOTATOC uptake derived from PET images, we could estimate the activity concentration of ^{90}Y-DOTATOC in the tumor during surgery to be equal to 4.8 kBq/ml.

^{90}Y ($T_{1/2} = 2.66$ days) decays mainly by beta minus emission with end point energy equal to 2.28 MeV and a small fraction of pair production. Because of the direct interaction with the CCD of bremsstrahlung and gamma rays emitted by ^{90}Y, a small sparse spike noise pattern is generated during the emission image acquisition. The spikes have been removed by applying a box median filter with a size equal to 3×3 pixels on the emission data.

The specimens of the tumor removed by the surgeon were imaged using both CLI and RLI as described before. The sample activity could not be directly measured simply because surgery was carried out in a hospital that did not have a nuclear medicine division with appropriate instrumentation. The sample has a dimension of $5 \times 11 \times 9$ mm^3; thus, the estimated activity was equal to 2.4 kBq.

Figure 2(a) shows the photographic picture of the tumor specimen, Fig. 2(b) the Cerenkov image, and Fig. 2(c) the RLI signal. The images confirm an appropriate localization of the visible Cerenkov and radioluminescence light signal within the tumor region.

To our knowledge, this is the first published experimental evidence of the possibility of detecting Cerenkov and radioluminescence light from a fresh human tumor specimen removed during surgery.

As expected, the detected light signal is higher in RLI with respect to CLI; we used the same color scale in order to provide a better comparison between CLI and RLI signals. A circular (3 mm diameter) region of interest was drawn at the center of the tumor specimen, and the mean value was calculated for both CLI and RLI. We found that the average values of the CLI and RLI signal were, respectively, equal to 582 and 652 (arbitrary units).

The higher background signal in RLI data around the specimen is due to direct interaction of the high-energy beta particles with the scintillator slab.

In summary, we showed, for the first time, examples of CLI and RLI images of a fresh human brain tumor specimen removed during neurosurgery of a patient previously administered, for investigational purposes, with 166 MBq of ^{90}Y-DOTATOC.

The FOV of 6.1×6.1 cm allows the acquisition of few surgical samples simultaneously, reducing the total time needed for the imaging process.

As shown by recent Monte Carlo simulation,[23] the use of ^{90}Y is ideal considering the higher number of Cerenkov photons emitted in the tissues with respect, for example, to ^{18}F.

The CLI signal of the specimen is well confined in the tumor region, while the RLI signal is higher but also contains higher
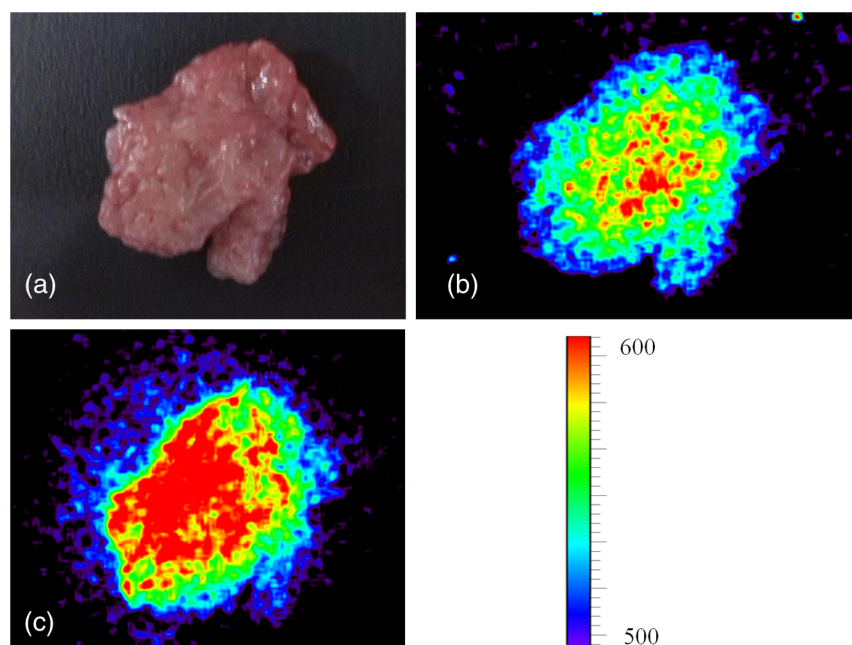
Fig. 2 (a) A color image evincing the amount of blood present in the tumor specimen, and (b) and (c) the CLI and RLI signals. As can be seen from the images in (b) and (c), there is a good agreement between the localization of the visible Cerenkov and radioluminescence light signal within the tumor region. The color scale is in arbitrary units.

background outside the sample. We can conclude that CLI is the best option when the Cerenkov signal is high enough to be clearly detected, while RLI can be a good alternative option when the Cerenkov light is low. More precisely, RLI can be the best imaging approach when the radiotracer uptake is low, when using isotopes with low Cerenkov light yield, or with end point energy below the Cerenkov threshold.

The approach presented in this work could provide a fast molecular imaging method for the estimation of tumor radiopharmaceutical uptake during surgical procedures using Cerenkov and radioluminescence light.

Acknowledgments

References

1. A. E. Spinelli et al., "Optical imaging using radioisotopes: a novel multimodal approach to molecular imaging," *Q J Nucl Med Mol Imaging* **56**, 279–289 (2012).
2. A. E. Spinelli and F. Boschi, "Novel biomedical applications of Cerenkov radiation and radioluminescence imaging," *Phys. Med.* **31**(2), 120–129 (2015).
3. F. Boschi and A. E. Spinelli, "Cerenkov luminescence imaging at a glance," *Curr. Mol. Imaging* **3**, 106–117 (2014).
4. R. Robertson et al., "Optical imaging of Cerenkov light generation from positron-emitting radiotracers," *Phys. Med. Biol.* **54**, N355–N365 (2009).
5. A. E. Spinelli et al., "Cerenkov radiation allows in vivo optical imaging of positron emitting radiotracers," *Phys. Med. Biol.* **55**, 483–495 (2010).
6. F. Boschi et al., "In vivo (18)F-FDG tumour uptake measurements in small animals using Cerenkov radiation," *Eur. J. Nucl. Med.* **38**, 120–127 (2011).
7. A. E. Spinelli et al., "Cerenkov radiation imaging of beta emitters: in vitro and in vivo results," *Nucl. Instrum. Methods Phys. Res. A* **648**, S310–S312 (2011).
8. A. E. Spinelli et al., "Multispectral Cerenkov luminescence tomography for small animal optical imaging," *Opt. Express* **19**, 12605–12618 (2011).
9. F. Boschi et al., "Optical imaging of alpha emitters: simulations, phantoms and in vivo results," *J. Biomed. Opt.* **16**(12), 126011 (2011).
10. A. E. Spinelli et al., "Optical imaging of Tc-99m based tracers, in vitro and in vivo results," *J. Biomed. Opt.* **16**(11), 116023 (2011).
11. M. Shimamoto et al., "Hybrid light imaging using Cerenkov luminescence and liquid scintillation for preclinical optical imaging in vivo," *Mol. Imaging Biol.*, 1–10 (2016).
12. A. E. Spinelli et al., "First human Cerenkography," *J. Biomed. Opt.* **18**(2), 020502 (2013).
13. H. Hu et al., "Feasibility study of novel endoscopic Cerenkov luminescence imaging system in detecting and quantifying gastrointestinal disease: first human results," *Eur. Radiol.* **25**(6), 1814–1822 (2015).
14. A. E. Spinelli, C. R. Gigliotti, and F. Boschi, "Unified approach for bioluminescence, Cerenkov, β, X and γ rays imaging," *Biomed. Opt. Express* **6**, 2168 (2015).
15. F. Collamati et al., "Toward radioguided surgery with β- decays: uptake of a somatostatin analogue, DOTATOC, in meningioma and high-grade glioma," *J. Nucl. Med.* **56**(1), 3–8 (2015).
16. M. Bartolomei et al., "Peptide receptor radionuclide therapy with (90)Y-DOTATOC in recurrent meningioma," *Eur. J. Nucl. Med. Mol. Imaging* **36**(9), 1407–1416 (2009).
17. L. Bodei et al., "Receptor-mediated radionuclide therapy with ^{90}Y-DOTATOC in association with amino acid infusion: a phase I study," *Eur. J. Nucl. Med. Mol. Imaging*. **30**(2), 207–216 (2003).
18. L. Bodei et al., "The joint IAEA, EANM, and SNMMI practical guidance on peptide receptor radionuclide therapy (PRRNT) in neuroendocrine tumours," *Eur. J. Nucl. Med. Mol. Imaging*. **40**(5), 800–816 (2013).
19. L. Bodei et al., "Peptide receptor radionuclide therapy for advanced neuroendocrine tumors," *Thorac. Surg. Clin.* **24**(3), 333–349 (2014).

20. A. Filice et al., "Radiolabeled somatostatin analogues therapy in advanced neuroendocrine tumors: a single centre experience," *J. Oncol.* **2012**, 320198 (2012).
21. S. Koukouraki et al., "Evaluation of the pharmacokinetics of 68Ga-DOTATOC in patients with metastatic neuroendocrine tumours scheduled for 90Y-DOTATOC therapy," *Eur. J. Nucl. Med. Mol. Imaging* **33**(4), 460–466 (2006).
22. M. Ö. Öksüz et al., "Peptide receptor radionuclide therapy of neuroendocrine tumors with (90)Y-DOTATOC: is treatment response predictable by pre-therapeutic uptake of (68)Ga-DOTATOC?," *Diagn. Interv. Imaging* **95**(3), 289–300 (2014).
23. F. Boschi, M. Pagliazzi, and A. E. Spinelli, "Cerenkov luminescence imaging of human breast cancer: a Monte Carlo simulations study," *J. Instrum.* **11**(03), C03032 (2016).